Molecular beam epitaxy approach to the graphitization of GaAs(100) surfaces

Paul J. Simmonds[a] and John Simon
Department of Electrical Engineering, Yale University, P.O. Box 208284, New Haven, Connecticut 06520-8284

Jerry M. Woodall
School of Electrical and Computer Engineering, Purdue University, 465 Northwestern Ave., West Lafayette, Indiana 47907-2035

Minjoo Larry Lee
Department of Electrical Engineering, Yale University, P.O. Box 208284, New Haven, Connecticut 06520-8284

(Received 27 October 2010; accepted 3 January 2011; published 25 January 2011)

The authors present a method for obtaining graphitized carbon on GaAs(100) surfaces. Carbon-doped GaAs is grown by molecular beam epitaxy before controlled thermal etching within the growth chamber. An AlAs layer beneath the carbon-doped GaAs acts as a thermal etch stop. As the GaAs is etched away, the carbon dopant atoms remain on the surface due to their low vapor pressure. The total number of carbon atoms available is precisely controllable by the doping density and thickness of the carbon-doped GaAs layer. Characteristic phonon modes in Raman spectra from the thermally etched surfaces show that the residual surface carbon atoms form sp^2-bonded graphitic crystallites. © *2011 American Vacuum Society.* [DOI: 10.1116/1.3547716]

I. INTRODUCTION

Graphene is a sheet of sp^2-bonded carbon, which is one monolayer thick. Deriving in part from the fact that electrons and holes in graphene behave as Dirac fermions, graphene displays many attractive properties, including ultrahigh mobility[1] and exhibition of the quantum Hall effect at room temperature.[2] Numerous potential applications for graphene have been proposed, including transistors[3,4] and electrical interconnects.[5] In this paper, we propose a method for the direct formation of graphene on GaAs(100) substrates using a molecular beam epitaxy (MBE)-based approach and provide evidence of surface graphitization using this technique.

Currently, the majority of epitaxial graphene is produced using one of two established techniques. The first is a chemical vapor deposition (CVD) process involving hydrocarbon gas flow across a metal substrate (commonly Ni or Cu).[6,7] At a substrate temperature (T_{SUB}) of ~950 °C, a carbon-rich solid solution is formed in the metal, close to the surface. Since the solid solubility of carbon in the metal decreases upon cooling, the carbon atoms segregate to the surface and form graphene. This CVD-based process has the advantage of close control over the number of graphene layers formed.[6] However the size of the graphene domains formed is limited by the extent of the metal grains.[6] In addition, the graphene sheet must typically be transferred from the metal surface to a suitable substrate for device fabrication.[7] The second approach involves the graphitization of SiC substrates by heating to T_{SUB}=1200–1400 °C in an inert environment.[8,9] Si atoms sublime from the surface, leaving excess carbon atoms behind. Graphitization ensues once the surface carbon concentration exceeds some threshold.[10] Although high-speed devices incorporating such layers have already been demonstrated,[11] disadvantages to this method include high substrate cost, rough starting SiC surfaces that lead to rough discontinuous graphene sheets,[12] a lack of control over the number of graphene layers formed, and the extremely high T_{SUB} required.

More recently, in an attempt to address some of the issues facing these established epitaxial graphene production methods, MBE-based carbon deposition techniques for graphitizing various substrates have been developed. Garcia *et al.* deposited carbon films onto Ni surfaces, substituting the CVD approach described above with the physical vapor deposition of carbon atoms from a graphite filament source.[13] Following annealing at 800–900 °C, graphene layers formed on the metal surface, ready for transfer to suitable substrates for device fabrication. Groups have also looked at modifying the SiC graphitization technique by essentially reversing the sublimation process. Instead of the removal of Si atoms via high temperature sublimation, carbon atoms are supplied to the SiC surface using either a graphite filament source[14,15] or C_{60} molecules from an effusion cell.[15] A third method, developed by Hackley *et al.*, does not derive directly from either of the established graphene epitaxy techniques but aims to form graphene directly on Si(111) substrates.[16] Carbon is supplied from an electron beam evaporator and a two-step annealing procedure is used to form graphitic material while suppressing the formation of SiC. These MBE-based approaches are beginning to yield promising results. However, an ideal technique for the production of cheap high-quality graphene has yet to be found.

We propose a method for the MBE-based formation of graphene on GaAs which is built upon three well-known and

[a]Electronic mail: p.j.simmonds.03@cantab.net

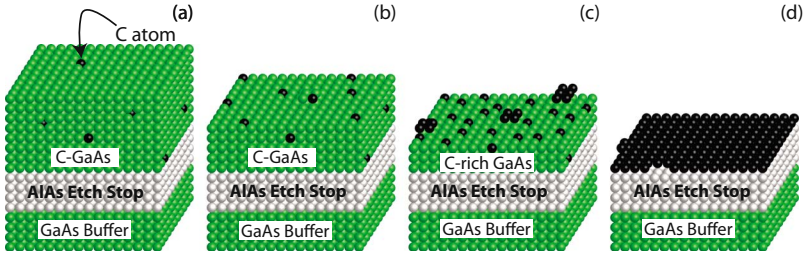

FIG. 1. (Color online) Schematic diagrams depicting the process of MBE-based graphene growth on GaAs. (a) Carbon-doped GaAs is grown above an AlAs etch-stop layer on a GaAs buffer. (b) Under an overpressure of As_2, T_{SUB} is raised such that GaAs etches away in a layer-by-layer fashion. (c) Carbon atoms remain on the surface due to very low vapor pressure at typical T_{SUB} and the GaAs surface becomes increasingly carbon rich. (d) Epitaxially flat AlAs acts as a thermal etch-stop layer once all the GaAs is removed, and a thin layer of carbon atoms is left on the surface.

experimentally observed processes. First, GaAs can be thermally etched in a layer-by-layer fashion. In this process, a GaAs surface is heated under an As_2 overpressure sufficient to prevent the formation of Ga droplets. Once T_{SUB} becomes high enough, Ga atoms begin to sublime from the surface.[17] Ga sublimation is precisely controllable, to the extent that it is possible to observe reflectance high-energy electron diffraction (RHEED) intensity oscillations corresponding to the removal of successive monolayers of GaAs.[18] This process is the direct antithesis of layer-by-layer MBE growth.[19] The second concerns the fact that in the temperature range used to thermally etch GaAs, AlAs undergoes negligible sublimation.[17] Third, it is possible to grow GaAs that is extremely heavily doped with carbon: Shirakashi *et al.* demonstrated GaAs with carbon-doping levels as high as 1.5×10^{21} cm^{-3}.[20]

Our method combines these three processes into a single technique. First, a GaAs buffer is grown by MBE onto a GaAs(100) substrate to provide a clean flat starting surface. A thin AlAs etch-stop layer is then grown, followed by a layer of heavily carbon-doped GaAs (GaAs:C) [Fig. 1(a)]. The sample is then heated under an As_2 flux such that the GaAs begins to thermally etch away [Fig. 1(b)]. Carbon has very low vapor pressure at typical Ga sublimation temperatures (650–750 °C) and so is left behind as the GaAs is etched [Fig. 1(c)].[21] Once all the GaAs has been removed, the AlAs layer acts as a thermal etch stop.[21] The residual carbon on the surface is expected to graphitize on the epitaxially smooth AlAs once the concentration exceeds some threshold, in an analogous fashion to the graphitization of SiC by Si sublimation.[10] The number of layers of graphene produced by this technique is dependent only on the number of carbon atoms available. A single monolayer of graphene consists of 3.8×10^{15} cm^{-2} carbon atoms, which is approximately equivalent to the total number of carbon atoms in a 2-μm-thick layer of GaAs:C doped to 2×10^{19} cm^{-3}. Due to the nature of the MBE growth technique, precise control over both the thickness and the doping density of the GaAs:C layer gives two degrees of freedom in dictating the number of available carbon atoms and hence the number of graphene layers.

We believe the approach presented here helps address some of the issues faced by current techniques for producing epitaxial graphene. These include the low cost of GaAs substrates compared with SiC, a smooth single crystal AlAs surface on which graphitization can occur, the precise control over the number of graphene layers formed, and the potential for use of the graphene directly on the semiconductor substrate without the need for transfer.

II. EXPERIMENT

All samples were grown in a Veeco GEN-II MBE system on GaAs(100) on-axis (±0.5°) substrates. We used *in situ* RHEED observations to study the surfaces of our samples during growth and thermal etching. After removal from the MBE chamber we used a Veeco atomic force microscope (AFM) to investigate the sample surface morphology. To characterize the chemical composition of the thermally etched GaAs surfaces, we performed Raman spectroscopy measurements in a HORIBA LabRAM 300 system, with a 532 nm wavelength incident laser and a 100× objective lens. A commercially available exfoliated graphene flake on SiO_2/Si was used as a Raman reference standard sample.

We first calibrated the thermal etch rate of GaAs as a function of T_{SUB}. A sequence of four undoped GaAs layers was grown, separated by $Al_{0.6}Ga_{0.4}As$ markers. Each GaAs layer was grown for 330 s at a nominal growth rate of 1 μm/h (measured at 580 °C) under a V/III beam equivalent pressure (BEP) ratio of ~15. The first 330 s GaAs layer was immediately capped with 15 nm $Al_{0.6}Ga_{0.4}As$. Following growth of the second 330 s GaAs layer, the surface was held at T_{SUB} under an As_2 overpressure of 1.6×10^{-5} Torr for 10 min (i.e., thermally etched) before capping with 15 nm $Al_{0.6}Ga_{0.4}As$. The third and fourth 330 s GaAs layers were thermally etched in identical fashion for 20 and 30 min, respectively, before growth of their 15 nm $Al_{0.6}Ga_{0.4}As$ caps. Growth of the sequence of four GaAs layers was repeated at five different values of T_{SUB}—580, 638, 670, 695, and 735 °C—to create a large GaAs/$Al_{0.6}Ga_{0.4}As$ stack. We then imaged the GaAs/$Al_{0.6}Ga_{0.4}As$ stack using cross-sectional transmission electron microscopy (XTEM) in a Tecnai T12 machine operated at 120 kV.

We used CBr_4 as the carbon source during MBE growth of GaAs:C. Carbon-doping density was calibrated using a combination of secondary ion mass spectroscopy and Hall-effect measurements. Using this approach we grew GaAs:C

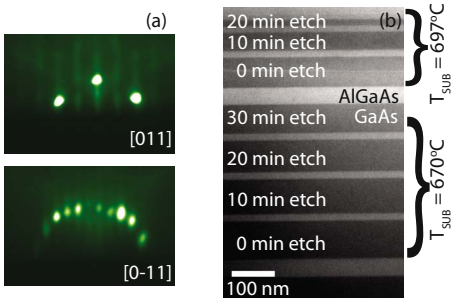

FIG. 2. (Color online) (a) RHEED patterns along orthogonal azimuths of an undoped GaAs etch-rate calibration stack sample at the end of growth, showing a 2×4 reconstructed surface. (b) Part of the cross-sectional transmission electron micrograph of the etch-rate calibration stack sample, consisting of a series of undoped GaAs layers grown and thermally etched at various values of T_{SUB} and separated by $Al_{0.6}Ga_{0.4}As$ markers.

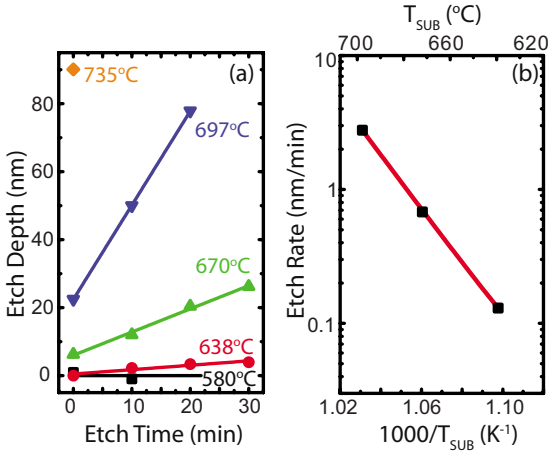

FIG. 3. (Color online) (a) GaAs thermal etch depth as a function of time at various values of T_{SUB}. (b) Arrhenius plot of thermal etch rate of undoped GaAs as a function of T_{SUB}.

doped as high as 6×10^{19} cm^{-3} with a corresponding room temperature hole mobility of ~80 $cm^2/V\,s$, indicating minimal carrier compensation.

To investigate the thermal etching and graphitization of GaAs:C we grew samples with the structure schematically represented in Fig. 1(a). At $T_{SUB}=590$ °C we grew a 500 nm GaAs buffer, followed by a 5 nm AlAs thermal etch-stop layer grown at $T_{SUB}=640$ °C. Then, at $T_{SUB}=590$ °C, we grew 2 μm of GaAs, doped to 2×10^{19} cm^{-3} with carbon. Samples were grown at 1 $\mu m/h$ under a V/III BEP ratio of ~15.

To initiate thermal etching following growth, we heated our GaAs:C samples in the MBE chamber to the required T_{SUB}. Etch rate is controlled primarily by T_{SUB}, with a weaker dependence on As_2 overpressure.[17] For this reason, all thermal etching of GaAs was carried out under the same As_2 overpressure of 1.6×10^{-5} Torr that we used in our etch-rate calibration.

III. RESULTS AND DISCUSSION

A. Thermal etch-rate calibration

The thermal etching of undoped GaAs proceeds in a layer-by-layer fashion, even at high T_{SUB}. At the end of growth of the $GaAs/Al_{0.6}Ga_{0.4}As$ etch-rate calibration stack described above, the sample exhibited a streaky 2×4 RHEED pattern [Fig. 2(a)]. This pattern indicates a smooth reconstructed surface despite the multiple etching and regrowth steps up to $T_{SUB}=735$ °C and hence a well-controlled thermal etch process.

We can control the thermal etch rate of undoped GaAs over more than two orders of magnitude as a function of T_{SUB}. The thickness of each GaAs layer in the $GaAs/Al_{0.6}Ga_{0.4}As$ growth-rate calibration stack was measured from XTEM images [Fig. 2(b)]. Using the thickness of the GaAs layer that had been immediately capped with $Al_{0.6}Ga_{0.4}As$ to represent a "zero etch time" for each etch temperature, we were able to plot GaAs etch depth against time for each value of T_{SUB} [Fig. 3(a)]. At $T_{SUB}=580$ °C, the GaAs thermal etch rate was below the sensitivity of the measurement technique. At $T_{SUB}=735$ °C, the thermal etch rate was comparable to the growth rate of 1 $\mu m/h$ and so the thickness of the net deposited GaAs was too thin to measure accurately. Negligible etching of the $Al_{0.6}Ga_{0.4}As$ marker layers was observed at the highest values of T_{SUB} used, validating the use of AlAs as a thermal etch-stop layer in later growths. From the slope of an Arrhenius plot of these data [Fig. 3(b)] we calculated an activation energy, $E_a\sim3.6$ eV, for the thermal etching of undoped GaAs, which is consistent with both experiment[22] and theory for arsenic-rich surfaces under an As_2 overpressure of $\sim2\times10^{-5}$ Torr.[23]

B. Thermal etching of GaAs:C

The presence of carbon atoms appears to strongly affect the GaAs thermal etch process. We heated a sample of GaAs:C to $T_{SUB}=735$ °C, corresponding to an etch rate of ~15 nm/min calculated from an extrapolation of the calibration curve in Fig. 3(b). This gave a total etch time for the 2 μm GaAs:C layer of ~130 min. Shortly after initiating the thermal etch of the GaAs:C, RHEED showed a change from a streaky 2×4 reconstruction to a spotty diffraction pattern, indicating surface roughening. This behavior was completely different from that observed during the controlled etching of undoped GaAs [Fig. 2(a)]. The GaAs:C surface showed no sign of smoothing as thermal etching proceeded.

AFM analysis of the sample surface following the thermal etch confirmed an extremely rough morphology and the absence of a continuous sheet of graphene [Fig. 4]. We speculate that the observed roughness is caused by nanoscopic graphitic crystallites forming at the surface once the Ga atoms begin to sublime. Once these crystallites reach a certain size they become stable, preventing underlying Ga atoms from leaving the surface and hence masking thermal etching of the GaAs below. To gain a better understanding of the thermal etch process and confirm this hypothesis we plan in the future to etch identical samples for various lengths of time to study how the GaAs:C surface evolves. By optimizing variables such as the GaAs:C doping density and the thermal etch conditions we hope to be able to better control

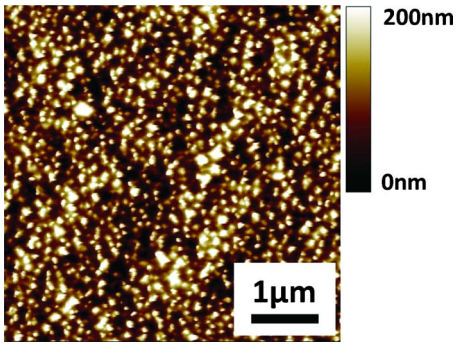

FIG. 4. (Color online) (5 μm)^2 AFM image showing the surface of a 2-μm-thick GaAs:C layer thermally etched at 735 °C. Root mean square roughness was measured to be ~25 nm over this area.

the morphology of the thermally etched surface and thereby increase the size of these crystallites toward large area graphene.

C. Raman spectroscopy of graphitized surfaces

Using Raman spectroscopy we identified the existence of graphitic carbon on the surfaces of thermally etched GaAs:C. The Raman spectrum of a standard sample of graphene exhibits characteristic D (~1345 cm^{-1}), G (~1589 cm^{-1}), and G' (also referred to as $2D$, ~2680 cm^{-1}) vibrational phonon modes, consistent with previous measurements of sp^2-bonded carbon for a 532 nm wavelength excitation laser (Fig. 5).[24] These three vibrational modes correspond, respectively, to the phonons at graphitic zone boundaries, the stretching of in-plane carbon-carbon bonds, and the second order mode of zone-boundary phonons.[16,25] We observed these phonon modes at 1338, 1604, and 2665 cm^{-1} in the Raman spectra from our thermally etched GaAs:C samples, with no signature peaks from sp^3-bonded carbon.[26] Despite their low intensity when compared with the graphene standard, the presence of these peaks confirms that the thermally etched GaAs:C surfaces have become graphitized to some extent.

The graphitic carbon on the surface appears to be highly disordered. In a Raman spectrum of graphene with high

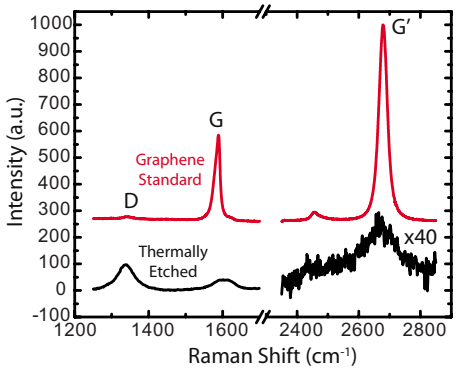

FIG. 5. (Color online) Raman spectra of the surface of GaAs:C thermally etched at T_{SUB}=735 °C (lower curves) compared with a graphene standard sample (upper curves) in the range of 1200–2900 cm^{-1}.

structural quality (see the spectrum from the graphene standard sample in Fig. 5 as an example), the G peak dominates, while the D peak is typically observed only in spectra measured at the edges of a graphene sheet.[25] Since D mode phonons are associated with edge defects, the relative strength of this peak in our Raman spectra suggests the presence of numerous graphitic domains. In addition, the small increase in the position of the G peak from 1589 cm^{-3} (for the graphene standard sample) to 1604 cm^{-1} (in the Raman spectrum from the thermally etched sample) has been previously shown to indicate nanocrystalline graphite.[26] These observations provide support for our belief that nanoscale graphitic crystallites are responsible for the roughness of our sample surfaces.

The ratio of the intensity of the D phonon mode (I_D) to that of the G phonon mode (I_G) tends to zero in highly ordered graphene.[27] The Raman peak intensity ratio (I_D/I_G) for the spectrum from our thermally etched GaAs:C sample in Fig. 5 was 2.94. We used I_D/I_G to calculate the average in-plane size (L_a) of the graphitic crystallites via[26,27]

$$L_a = C(\lambda_L)\left(\frac{I_D}{I_G}\right)^{-1}. \quad (1)$$

The dependence of the Raman coupling coefficient $C(\lambda_L)$ on the excitation laser wavelength λ_L is given to the first order by the relation

$$C(\lambda_L) \approx C_0 + \lambda_L C_1. \quad (2)$$

Matthews *et al.*[28] obtained experimental values for the two fitting constants of C_0=−126 Å and C_1=0.033 which, when applied to our experimental setup, gives us a value of C(532 nm)≈50 Å. Using I_D/I_G=2.94 in Eq. (1), we then obtain an average size of 1.7 nm for the graphitic crystallites on our thermally etched sample. The size of these graphitic crystallites is comparable to those reported previously for the graphitization of Si(111) substrates.[16] However, Juang *et al.* recently obtained graphene sheets of a few microns in size using an alternative low temperature (≤750 °C) technique based on the diffusion of carbon atoms through a thin Ni layer from SiC.[29] Their work shows that larger area graphene formation is achievable close to the value of T_{SUB} we have investigated and demonstrates therefore the need for optimization of our thermal etch process.

IV. SUMMARY AND CONCLUSIONS

We have demonstrated a technique for the graphitization of GaAs(100) surfaces. Carbon-doped GaAs is grown on an AlAs etch-stop layer. After thermally etching the GaAs:C within the MBE growth chamber under an As_2 overpressure, we verified the presence of graphitic material using Raman spectroscopy. Future work will focus on optimizing the doping and thermal etch conditions to improve the uniformity of the GaAs:C etch and yield larger graphitic domain sizes.

ACKNOWLEDGMENTS

The authors thank Andy Jackson (UCSB) for many helpful discussions. Two of the authors (P.J.S. and J.S.) contributed equally to this work.

[1]K. Bolotin, K. Sikes, Z. Jiang, M. Klima, G. Fudenberg, J. Hone, P. Kim, and H. Stormer, Solid State Commun. **146**, 351 (2008).
[2]K. Novoselov *et al.*, Science **315**, 1379 (2007).
[3]Qin Zhang, Tian Fang, Huili Xing, A. Seabaugh, and D. Jena, IEEE Electron Device Lett. **29**, 1344 (2008).
[4]L. Liao *et al.*, Nature (London) **467**, 305 (2010).
[5]R. Murali, K. Brenner, Yinxiao Yang, T. Beck, and J. Meindl, IEEE Electron Device Lett. **30**, 611 (2009).
[6]A. Reina, X. Jia, J. Ho, D. Nezich, H. Son, V. Bulovic, M. S. Dresselhaus, and J. Kong, Nano Lett. **9**, 30 (2009).
[7]K. S. Kim *et al.*, Nature (London) **457**, 706 (2009).
[8]C. Berger *et al.*, Science **312**, 1191 (2006).
[9]E. Rollings *et al.*, J. Phys. Chem. Solids **67**, 2172 (2006).
[10]I. Forbeaux, J. Themlin, and J. Debever, Phys. Rev. B **58**, 16396 (1998).
[11]C. Dimitrakopoulos *et al.*, J. Vac. Sci. Technol. B **28**, 985 (2010).
[12]J. Robinson *et al.*, ACS Nano **4**, 153 (2010).
[13]J. M. Garcia *et al.*, Solid State Commun. **150**, 809 (2010).
[14]E. Moreau, F. J. Ferrer, D. Vignaud, S. Godey, and X. Wallart, Phys. Status Solidi A **207**, 300 (2010).
[15]J. Park, W. C. Mitchel, L. Grazulis, H. E. Smith, K. G. Eyink, J. J. Boeckl, D. H. Tomich, S. D. Pacley, and J. E. Hoelscher, Adv. Mater. **22**, 4140 (2010).
[16]J. Hackley, D. Ali, J. DiPasquale, J. D. Demaree, and C. J. K. Richardson, Appl. Phys. Lett. **95**, 133114 (2009).
[17]J. M. Van Hove and P. I. Cohen, Appl. Phys. Lett. **47**, 726 (1985).
[18]T. Kojima, N. J. Kawai, T. Nakagawa, K. Ohta, T. Sakamoto, and M. Kawashima, Appl. Phys. Lett. **47**, 286 (1985).
[19]W. T. Tsang, T. H. Chiu, and R. M. Kapre, Appl. Phys. Lett. **63**, 3500 (1993).
[20]J. Shirakashi, T. Azuma, F. Fukuchi, M. Konagai, and K. Takahashi, Jpn. J. Appl. Phys., Part 1 **34**, 1204 (1995).
[21]A. C. Warren, J. M. Woodall, E. R. Fossum, G. D. Pettit, P. D. Kirchner, and D. T. McInturff, Appl. Phys. Lett. **51**, 1818 (1987).
[22]J. Reithmaier, R. F. Broom, and H. P. Meier, Appl. Phys. Lett. **61**, 1222 (1992).
[23]R. Heckingbottom, J. Vac. Sci. Technol. B **3**, 572 (1985).
[24]R. P. Vidano, D. B. Fischbach, L. J. Willis, and T. M. Loehr, Solid State Commun. **39**, 341 (1981).
[25]A. C. Ferrari *et al.*, Phys. Rev. Lett. **97**, 187401 (2006).
[26]A. C. Ferrari and J. Robertson, Phys. Rev. B **61**, 14095 (2000).
[27]F. Tuinstra and J. Koenig, J. Chem. Phys. **53**, 1126 (1970).
[28]M. J. Matthews, M. A. Pimenta, G. Dresselhaus, M. S. Dresselhaus, and M. Endo, Phys. Rev. B **59**, R6585 (1999).
[29]Z. Juang, C. Wu, C. Lo, W. Chen, C. Huang, J. Hwang, F. Chen, K. Leou, and C. Tsai, Carbon **47**, 2026 (2009).